ELSEVIER

Ceramics International 29 (2003) 145–150

CERAMICS INTERNATIONAL

www.elsevier.com/locate/ceramint

Dielectric and piezoelectric properties for $0.62Pb(Mg_{1/3}Nb_{2/3})O_3$–$0.38PbTiO_3$ single crystals

Hu Cao, Bijun Fang, Haosu Luo*, Yihai Sun, Jingkun Guo

The State Key Laboratory of High Performance Ceramics and Superfine Microstructure, Shanghai Institute of Ceramics, Chinese Academy of Sciences, 215 Chengbei Road, Jiading, Shanghai 201800, China

Received 16 January 2002; received in revised form 16 March 2002; accepted 20 May 2002

Abstract

The dielectric and piezoelectric properties of $0.62Pb(Mg_{1/3}Nb_{2/3})O_3$–$0.38PbTiO_3$ single crystal (PMNT62/38) were investigated in this work. Power X-ray diffraction demonstrated PMNT62/38 had a tetragonal structure at room temperature. The Curie temperature was 187 °C on heating. The poled and as-grown dielectric constants ε_r of [001] oriented PMNT62/38 at room temperature were ~500 and ~5000, respectively. The remanent polarization P_r and coercive field E_c for [001] oriented one were 34.2 μC/cm^2 and 8.25 kV/cm, respectively. The strain at 15 kV/cm and −15k V/cm were 0.078 and 0.125%, respectively. The piezoelectric constant d_{33} was ~350 pC/N. The electromechanical coupling coefficients; 0.89 of k_{33}, 0.61 of k_t, 0.46 of k_{31} and 0.45 of k_{15} were calculated from measured resonance and anti-resonance frequencies by impedance resonance techniques. In single domain process it was found the re-oriented domains of [001] poled PMNT62/38 were instable, which caused it hard to align the spontaneous polarizations to create a single domain crystal.

Keywords: C. Dielectric properties; C. Piezoelectric properties; Lead magnesium niobate titanate

1. Introduction

More recently, relaxor-based ferroelectric single crystals, $(1-x)Pb(Mg_{1/3}Nb_{2/3})O_3-xPbTiO_3$ (PMNT), due to their broad composition range and very high dielectric and piezoelectric properties, electromechanical coupling coefficients and field-induced strain response [1], have come into prominence in contrast to conventional PZT family of ceramics. For instance, PMNT67/33 single crystal, have large piezoelectric constant (d_{33}~2000 pC/N), dielectric constant (ε_r~5000) and electromechanical coupling factor (k_{33}~94%) [1]. Some applications, such as the ultrasonic imaging, sonar and actuator are based on these large coefficients of the material.

PMNT single crystals with complex perovskite structure are cubic phase (m3m) above their Curie temperature (T_c) and rhombohedral (3m) or tetragonal phase (4 mm) below T_c, depending on the value of x. There is a morphotropic phase boundary (MPB) around $x=0.33\sim0.35$, where they exhibit optimum piezoelectric properties. The $0.62Pb(Mg_{1/3}Nb_{2/3})O_3$–$0.38PbTiO_3$ (PMNT62/38), which deviates from the MPB, is expected to be tetragonal phase at room temperature and the spontaneous polarization is along the $<001>$ direction (c-axis). In this paper, we will report in details the dielectric and piezoelectric properties of PMNT62/38 in order to investigate the properties of tetragonal PMNT single crystals.

Most oxygen-octahedra ferroelectrics, which exhibit excellent electromechanical properties, generally also have the outstanding optical properties [2,3]. PMNT single crystals have giant piezoelectric constants and electromechanical coupling coefficients and are expected to have excellent optical properties. However, before used as optical materials they should be made single domain. Samples cut from the boule of PMNT62/38 single crystals are multi-domains in structure. This is, the samples consist of regions that have their own polar axes (spontaneous polarization) perpendicular or antiparallel with respect to each other. Therefore, multidomains must be eliminated through aligning the spontaneous polarizations everywhere in crystals to create a

* Corresponding author.
E-mail address: hsluo@public3.sta.net.cn (H. Luo).

0272-8842/03/$22.00
PII: S0272-8842(02)00098-6

single domain crystal. In this paper we will also report some work on single domain process.

2. Experimental procedure

Ferroelectric single crystals PMNT62/38 were grown by the modified Bridgman technique [4,5]. The boule of PMNT62/38 crystal was cut along the pseudocubic crystallographic face (100) determined by an X-ray diffractometer. Four different Z-cut samples, possessing appropriate aspect ratios as determined by IEEE Standards [6], were prepared for dielectric constant, piezoelectric and electromechanical coupling coefficients and $6\times6\times6$ mm^3 cubes with six {100} faces were prepared for single domain process. The Z-cut samples and the cubic samples were poled under an electric field of 1 kV/mm for 15 min at 170 °C in silicon oil and cooled to room temperature with the half of the applied electric field. The cubic samples, after electric poling, any surface damage at the electrode was removed with 9 μm Al_2O_3-grit. Then the crystal is polished with 3 μm diamond paste.

The phase structure of PMNT62/38 crystal was determined by powder X-ray diffraction. The HP4192A impedance analyzer was used to measure the dielectric constants as a function of temperature on heating and on cooling at the frequency of 100 Hz to 100 kHz. The resonance and anti-resonance frequencies, which were used to calculate the values of k_{33}, k_t, k_{31} and k_{15} were measured by HP4192A. The P–E hysteresis loop was measured with Sawyer–Tower method at a frequency of 1 Hz and the strain versus the electric field curve was obtained using a linear variable differential transducer (LVDT). The domain patterns were observed by a polarized light microscope.

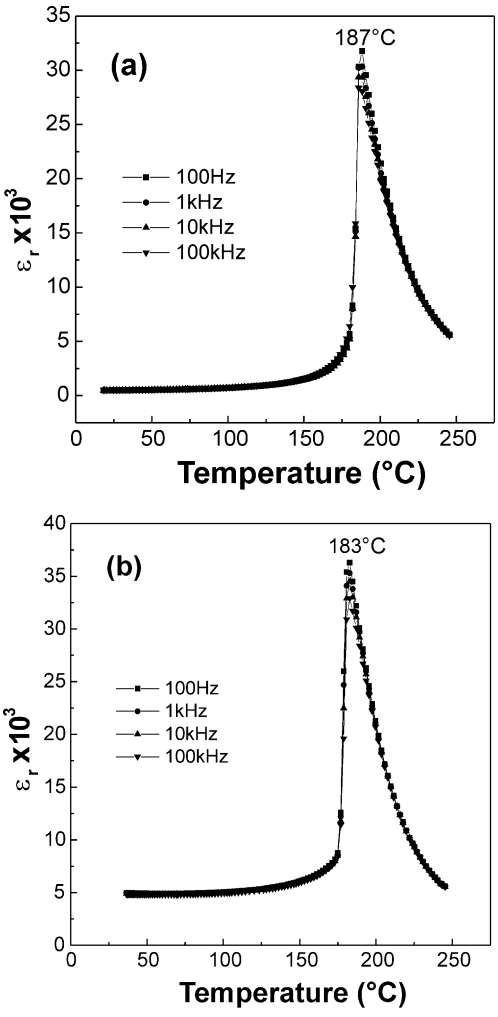

Fig. 1. Temperature and frequency dependence of dielectric constant ϵ_r for [001] oriented PMNT62/38 crystal. (a) For the poled plate on heating and (b) for the as-grown plate on cooling.

3. Results and discussion

3.1. Dielectric and piezoelectric properties

Fig. 1(a) and 1(b) show the dielectric constants as a function of temperature and frequency for [001] poled PMNT62/38 crystal on heating and cooling, respectively. The result of powder X-ray diffraction shows that the PMNT62/38 crystal, where the PT content is larger than that of PMNT crystals near the MPB, has a tetragonal phase at room temperature (Fig. 2). The crystal exhibits very little frequency dispersion in the dielectric constants whether on heating or on cooling over the measured temperature range. The real part of the dielectric permittivity ε_r exhibits a sharp change near the transition temperature 187 °C on heating and 183 °C on cooling. Thus, PMNT62/38 crystal is normal ferroelectrics and possesses the first-order phase transition at $T_c\sim187$ °C on heating from the tetragonal ferroelectric phase (FE_T) to the cubic paraelectric phase (PE_C) and at $T_c\sim183$ °C on cooling from PE_C to FE_T phase.

The piezoelectric constant d_{33} for [001] poled PMNT62/38 crystal is ~350 pC/N. The values of ε_r (poled) and ε_r (as-grown) at room temperature are ~500 and ~5000, respectively. PMNT62/38 crystal has the tetragonal phase at room temperature and the spontaneous polarization is along the $<001>$ direction. When crystals cooling through T_c, spontaneous polarizations in crystals are statistically along the six pseudocubic {100} faces, in response to the temperature gradients and mechanical stresses to maintain electrical neutrality of the crystals. Thus, 90 and 180°domains form and the domain walls are along $<110>$. Under the poling field along [001], the dipoles switch along the direction of the electric field, which results in the domains re-orienting. As a result, the single-domain regions increase and the volume of domain walls

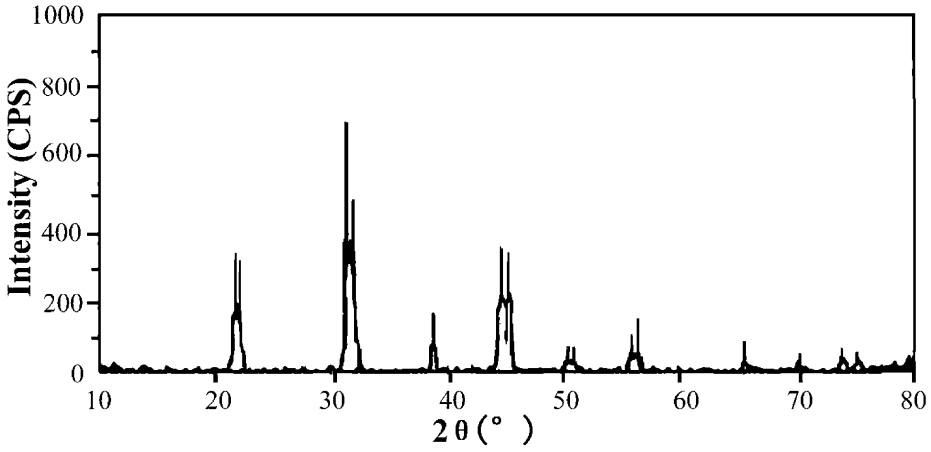

Fig. 2. Powder X-ray diffraction for PMNT62/38 crystal.

decrease, which cause the dielectric constants of poled samples are much less than that of as-grown ones.

3.2. Electromechanical coupling coefficients

The electromechanical coupling coefficients; k_{33}, k_t, k_{31} and k_{15} of PMNT62/38 crystal are calculated from the measured resonance and anti-resonance frequencies of length extensional mode of thin rod, thickness mode of thin square plate, lateral length extensional mode of bar and thickness shear mode of thin plate, respectively. Fig. 3 shows the plot of the real part of admittance and impedance versus frequency for length extensional mode of thin rod. The value of k_{33} can be calculated from the measured values of f_r and f_a using the equation,

$$k_{33}^2 = \frac{\pi f_r}{2f_a}\tan\left\{\frac{\pi(f_a\text{-}f_r)}{2f_a}\right\},$$

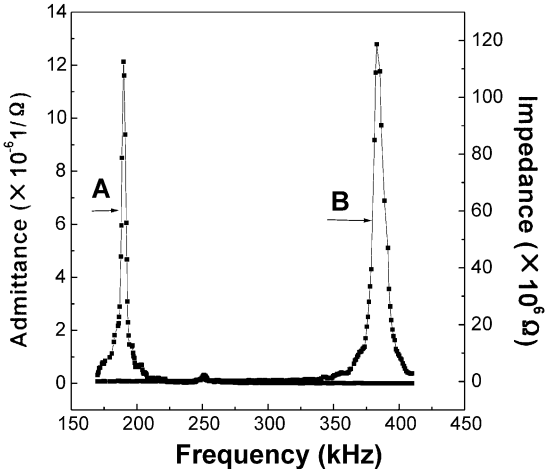

Fig. 3. Real part of admittance (A) and impedance (B) versus frequency for the length extensional mode of thin rod poled along [001] to determine the electromechanical coupling coefficient k_{33} for PMNT62/38 crystal.

where the anti-resonance frequency f_a is equal to the frequency of the largest value of the real part of impedance and the resonance frequency f_r is equal to the frequency of the smallest value of the real part of impedance, which can be considered approximately equal to the frequency of the largest value of the real part of admittance. In Fig. 3 the real part of admittance and impedance have the largest values at the frequency 190 and 386 kHz, respectively. Then, 0.89 of k_{33} was calculated using the earlier equation. Alike, the values of k_t, k_{15} and k_{31} were calculated from measured values of f_r and f_a using the given equations, respectively,

$$k_t^2 = \frac{\pi f_r}{2f_a}\tan\left\{\frac{\pi(f_a - f_r)}{2f_a}\right\}$$

$$k_{15}^2 = \frac{\pi f_r}{2f_a}\tan\left\{\frac{\pi(f_a - f_r)}{2f_a}\right\}$$

$$\frac{k_{31}^2 - 1}{k_{31}^2} = \frac{\tan\{(\pi/2)(f_a/f_r)\}}{(\pi/2)(f_a/f_r)}.$$

Table 1 presents the dimensions of samples, resonance and anti-resonance frequencies and electromechanical coupling coefficients for different vibrational modes.

3.3. Effect of electric field

Polarization hysteresis loop as a function of the electric field is presented in Fig. 4. The value of remanent polarization P_r is 34.2 μC/cm^2 and the value of coercive field E_c is 8.25 kV/cm when the electric field was applied to 15 kV/cm. By comparison, the [001] oriented PMNT67/33 and PMNT65/35 have 31 and 33 μC/cm^2 ofP_r [7]. The coercive field E_c goes from 3.5 kV/cm for [001] oriented PMN67/33 to 3.6kV/cm for [001] oriented PMNT65/35 [7] to 8.25 kV/cm for PMNT62/38. Due to the difference of polarization orientations between the

Table 1
Electromechanical coupling coefficients of PMNT62/38 crystal calculated from measured values of resonance and anti-resonance frequencies for different vibrational modes

Vibrational mode	Dimensions (mm) (l×w×t)	Frequency (Hz)		Electromechanical coupling coefficients
		f_r	f_a	
Length extension	7.3×1×1	1.90E+05	3.86E+05	$k_{33}=0.89$
Thickness shear	7.6×6.9×0.6	2.23E+06	2.46E+06	$k_{15}=0.46$
Lateral length extension	22.5×2.9×0.5	7.21E+04	7.87E+04	$k_{31}=0.45$
Thickness	10×9.3×0.5	3.63E+06	4.41E+06	$k_t=0.61$

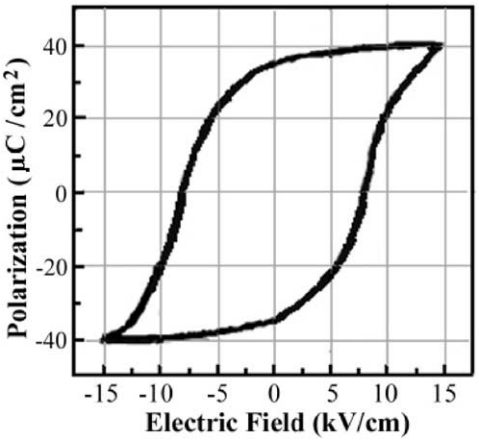

Fig. 4. *P–E* hysteresis loop as a function of the electric field for [001] oriented PMNT62/38 crystal; $P_r \sim 34.2\ \mu C/cm^2$ and $E_c \sim 8.25$ kV/cm.

tetragonal and rhombohedral PMNT crystals (the polarization orientation is along $<001>$ for tetragonal PMNT crystals, whereas it is along $<111>$ for rhombohedral ones), we cannot explain the E_c dependence on the PT content. However, according to the comparison earlier it seems that the E_c of polarization orientation is larger than those of non-polarization orientations. In order to confirm this case, the E_c of [110] and [111] oriented PMNT62/38 were also measured, ~6.8 and ~4.1 kV/cm respectively, less than $E_{c<001>}$ of 8.25kV/cm. The similar case happened to the PZN crystals, 3.8kV/cm of $E_{c<111>}$ and 2.7kV/cm of $E_{c<001>}$ [8]. The strain versus the electric field (bipolar) behavior for the [001] oriented PMNT62/38 is plotted in Fig. 5. The strain at 15 and −15kV/cm are 0.078 and 0.125%, respectively. The crystal has large strain hysteresis with applied bipolar electric field and the strain versus electric field curve is asymmetric. It is well known that the structural defects such as vacancy and microcracks in crystals tend to impede the domain motion, resulting in the localized electric field. The localized electric field cannot switch as the applied bipolar electric field, which influences the strain versus electric field behavior, therefore contributing to explain the asymmetry of strain behavior at bipolar electric field.

4. Single domain process

The domain structure in PMNT single crystals arises during first-order phase transition of PE_C to FE_T, serving to minimize free energy of a crystal. There are two types of domain patterns for tetragonal PMNT62/38, 90 and 180° domains, which are shown in the Fig. 6. The 180 and 90° domains play different roles to minimize the free energy. It has been accepted that in actual crystals of finite dimensions, 180° domains (the electric twins) and 90° domains (the mechanical twins) are distinguished according to their origin. The 180° domains arise so as to minimize the depolarizing field, whereas the 90° domains is required to compensate for the mechanical stress fields due to crystal imperfections [9,10], which disturb uniform domain structure and render it metastable. Here we adopt the conventional uniaxial pressing technique [11]. The 180° domains can be aligned parallel by heating the sample to near 170 °C and then applying an electric field greater than the

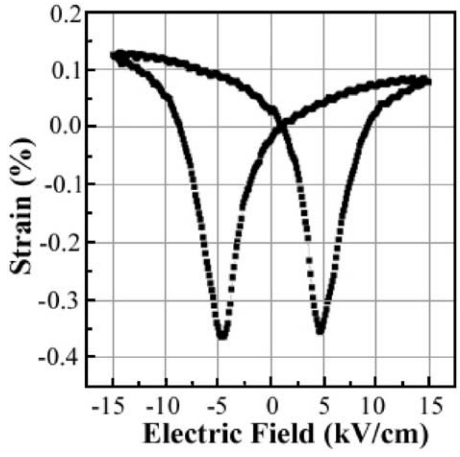

Fig. 5. Strain as a function of the electric field (bipolar) for the [001] oriented PMNT62/38 crystal. The strain is 0.078% at 15 kV/cm and 0.125% at −15 kV/cm.

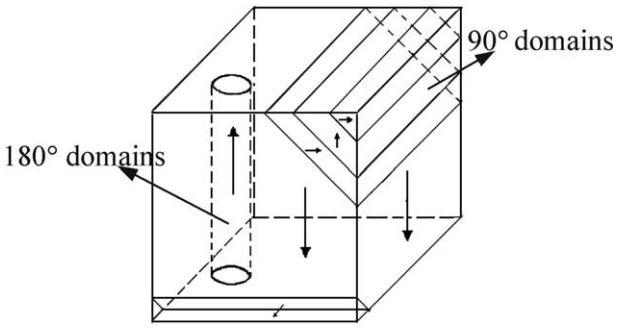

Fig. 6. Illustration of domains that form in the tetragonal PMNT62/38 crystal. These two types of domains, 90 and 180°, form in response to temperature gradients and mechanical stresses to maintain electrical neutrality of the sample when cooling through the Curie temperature. The polar axis for each domain is shown in the figure.

coercive field until room temperature. The elimination of 90 domains can be transiently accomplished by uniaxial pressing on (100) or (010) surfaces of the sample poled along [001]. Under the poling field the domains are aligned along the direction of electric field as much as possible. However, due to defects and stress in crystals, the domains can't completely switch along the electric field. After each pressing many but not all of the 90° domains are generally eliminated. The pressing of the sample causes internal displacement of atoms, which is translated to the surface and produces a surface displacement or "surface steps". The surface displacement must be eliminated by polishing before next pressing of the sample since they mechanically limit or "pin" the displacement of the atoms on the surface. After polishing the six surfaces to eliminate the surface steps the sample is pressed again on (100) or (010) surfaces. The process of polishing–pressing often has to be repeated many times.

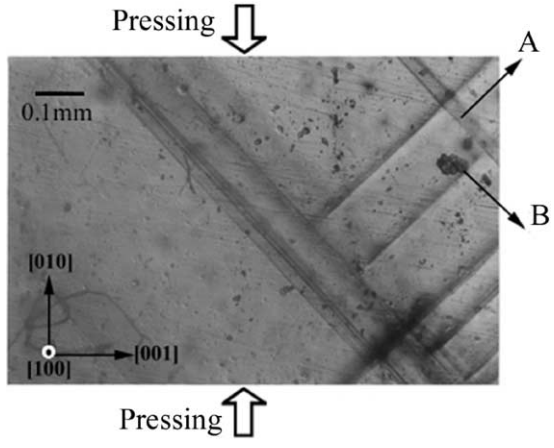

Fig. 7. The microstructure of 90° domains taken by a polarizing light microscope in the [001] poled cubic PMNT62/38 crystal ($6\times6\times6mm^3$) after pressed and polished on (100) or (010) surfaces. A and B are the crossed 90° domains walls along [110].

Fig. 7 shows the microstructure of 90° domains in the [001] poled cubic sample of PMNT62/38, after pressed and polished on (100) or (010) surfaces. Ninety degree domain walls are along [110]. A and B are intersected 90° domain walls. When the crystal is squeezed between one's fingers along [100] or [010] 90° domain walls gradually disappear along [110] and then pin up in (001) or (010) surfaces, hard to eliminate. After leaving it along for a while 90° domain walls come back to multi-domain status again just as shown the Fig. 7. This evidences show that the re-oriented domains are instable. Under the slight disturbance of temperature or stress, the re-oriented domains come back multi-domain status, accompanied the releasing of strain energy stored during the process of pressing.

5. Conclusion

Relaxor-based ferroelectric single crystals $0.62Pb(Mg_{1/3}Nb_{2/3})O_3$–$0.38PbTiO_3$ (PMNT62/38) can be grown directly from melt by a modified Bridgman technique. At room temperature it has tetragonal structure and the spontaneous polarization is along the $<001>$ direction. The sharp ε_r-T peak at Curie temperature and very little frequency dispersion in the dielectric constants, whether on heating or on cooling over the measured temperature range, indicate that the PMNT62/28 crystal is normal ferroelectrics and has a first-order character. The piezoelectric constant d_{33} is $\sim$350 pC/N. The electromechanical coefficients 0.89 of k_{33}, 0.61 of k_t, 0.46 of k_{31} and 0.45 of k_{15} are determined by impedance resonance techniques. The remnant polarization P_r is 34.2 $\mu C/cm^2$ when the electric field is applied to 15 kV/cm. Along the polarization orientation the coercive field show the maximum value of $E_{c<001>}\sim$8.25 kV/cm, larger than $\sim$6.8 kV/cm of $E_{c<110>}$ and $\sim$4.1k V/cm of $E_{c<111>}$.

Through the work about single domain process, we find that the re-oriented domains in [001] poled PMNT62/38 crystal are instable. With the process of pressing–polishing the 90° domain walls can disappear. However under the disturbance of temperature and stress, they still come back to multi-domain status. It should be adopted new methods in order to create a single domain crystal.

Acknowledgements

This project was supported by National Science Foundation of China (Grant No. 59995520) and the Shanghai Municipal Government (Grant No. 99XD14024).

References

[1] S.E. Park, T.R. Shrout, IEEE Trans. Ultrason. Ferroelectr. & Freq. Control 44 (1997) 1140–1147.
[2] M. DrDomenico Jr., S.H. Wemple, J. Appl. Phys. 40 (1969) 720–734.
[3] S.H. Wemple, M. DrDomenico Jr., J. Appl. Phys. 40 (1969) 735–752.
[4] Z. Yin, H. Luo, P. Wang, G. Xu, Ferroelectrics 299 (1999) 207–216.
[5] H. Luo, G. Xu, P. Wang, Z. Yin, Ferroelectrics 231 (1999) 97–102.
[6] "IEEE Std 176–1987," IEEE Standard on Piezoelectricity, IEEE Press, New York, 1987.
[7] G. Xu, H. Luo, P. Wang, Z. Qi, Z. Yin, Chinese Sci. Bull. 45 (6) (2000) 491–495.
[8] S.E. Park, T.R. Shrout, J. Appl. Phys. 82 (1997) 1804–1811.
[9] G.A. Smolensky, V.A. Bokov, V.A. Isupov, et al., Fizika segnetoelektricheskikh yavlenii, Nauka, Leningrad, 1985.
[10] I.S. Zheludev, Osnovy segnetoelektrichestva, Atomizdat, Moscow, 1973.
[11] M.H. Grrett, J.Y. Chang, H.P. Jenssen, C. Warde, Ferroelectrics 120 (1991) 167–173.